Chinese Physics Letters

EXPRESS LETTER

Anisotropic Superconducting Properties of Kagome Metal CsV_3Sb_5

To cite this article: Shunli Ni *et al* 2021 *Chinese Phys. Lett.* **38** 057403

CHIN. PHYS. LETT. Vol. 38, No. 5 (2021) 057403 **Express Letter**

Anisotropic Superconducting Properties of Kagome Metal CsV_3Sb_5

Shunli Ni(倪顺利)[1,2†], Sheng Ma(马晟)[1,2†], Yuhang Zhang(张宇航)[1,2†], Jie Yuan(袁洁)[1,2,5], Haitao Yang(杨海涛)[1,2,3,5*], Zouyouwei Lu(鲁邹有为)[1,2], Ningning Wang(王宁宁)[1,2], Jianping Sun(孙建平)[1,2], Zhen Zhao(赵振)[1,2], Dong Li(李栋)[1,2], Shaobo Liu(刘少博)[1,2], Hua Zhang(张华)[1,2], Hui Chen(陈辉)[1,2,3,5], Kui Jin(金魁)[1,2,5], Jinguang Cheng(程金光)[1,2], Li Yu(俞理)[1,2,5*], Fang Zhou(周放)[1,2,5], Xiaoli Dong(董晓莉)[1,2,5*], Jiangping Hu(胡江平)[1,4], Hong-Jun Gao(高鸿钧)[1,2,3,5], and Zhongxian Zhao(赵忠贤)[1,2,5]

[1]*Beijing National Laboratory for Condensed Matter Physics and Institute of Physics, Chinese Academy of Sciences, Beijing 100190, China*
[2]*University of Chinese Academy of Sciences, Beijing 100049, China*
[3]*CAS Center for Excellence in Topological Quantum Computation, University of Chinese Academy of Sciences, Beijing 100190, China*
[4]*Kavli Institute of Theoretical Sciences, University of Chinese Academy of Sciences, Beijing 100190, China*
[5]*Songshan Lake Materials Laboratory, Dongguan 523808, China*

(Received 2 April 2021; accepted 17 April 2021; published online 21 April 2021)

We systematically measure the superconducting (SC) and mixed state properties of high-quality CsV_3Sb_5 single crystals with $T_c \sim 3.5$ K. We find that the upper critical field $H_{c2}(T)$ exhibits a large anisotropic ratio of $H_{c2}^{ab}/H_{c2}^{c} \sim 9$ at zero temperature and fitting its temperature dependence requires a minimum two-band effective model. Moreover, the ratio of the lower critical field, H_{c1}^{ab}/H_{c1}^{c}, is also found to be larger than 1, which indicates that the in-plane energy dispersion is strongly renormalized near Fermi energy. Both $H_{c1}(T)$ and SC diamagnetic signal are found to change little initially below $T_c \sim 3.5$ K and then to increase abruptly upon cooling to a characteristic temperature of ∼2.8 K. Furthermore, we identify a two-fold anisotropy of in-plane angular-dependent magnetoresistance in the mixed state. Interestingly, we find that, below the same characteristic $T \sim 2.8$ K, the orientation of this two-fold anisotropy displays a peculiar twist by an angle of 60° characteristic of the Kagome geometry. Our results suggest an intriguing superconducting state emerging in the complex environment of Kagome lattice, which, at least, is partially driven by electron-electron correlation.

DOI: 10.1088/0256-307X/38/5/057403

Quasi-two-dimensional (2D) transition-metal Kagome systems serve as an important playground to study various electronic phenomena in the presence of geometric frustration and nontrivial band topology.[1−12] They can host frustrated magnetism, anomalous Hall effect, and various charge orders. The newly discovered AV_3Sb_5 (A = K, Rb, Cs) is a new class of Kagome family showing bulk superconductivity at T_c up to 2.5 K.[13−15] Some experimental results suggest unconventional pairing nature in such a Kagome system.[13,16−19] In addition, an exotic charge density wave (CDW)-like order can be identified at $T^* \sim$ 78–104 K in the normal state,[11,13−15,18,20−26] and coexists with the superconductivity at lower temperatures. The chirality of such a charge order is further verified by scanning tunneling microscopy (STM) measurements,[18,20,24,26] which can partially explain the giant anomalous Hall effect (AHE) in the system.[23,27] Recent transport measurements under pressure reveal that a superconducting dome appears as the charge order is suppressed by pressure.[17,21,22,28,29] All these findings suggest the rich and novel physics behind the superconductivity in the AV_3Sb_5 system. However, a systematic characterization of the fundamental superconducting (SC) properties such as lower/upper critical fields (H_{c1}/H_{c2}), mixed-state scattering characteristics, magnetic penetration depth (λ), and coherence length (ξ) is still lacking.

In this Letter, we present systematic magnetic and electrical transport measurements of high-quality single crystals of CsV_3Sb_5 showing a higher $T_c \sim 3.5$ K than the previous reports. The upper critical field exhibits a large anisotropic ratio H_{c2}^{ab}/H_{c2}^{c} up to 9 at zero temperature, and the fitting to the $H_{c2}(T)$ data requires a minimum two-band effective model. These are consistent with the quasi-2D and multiband nature[23,27] reported previously. Nevertheless, the lower critical field along ab-plane (H_{c1}^{ab}) is found to be higher than that along c-axis (H_{c1}^{c}). The

Supported by the National Natural Science Foundation of China (Grant Nos. 11834016, 11888101, 12061131005, 51771224 and 61888102), the National Key Research and Development Projects of China (Grant Nos. 2017YFA0303003 and 2018YFA0305800), the Key Research Program and Strategic Priority Research Program of Frontier Sciences of the Chinese Academy of Sciences (Grant Nos. QYZDY-SSW-SLH001, XDB33010200 and XDB25000000).
†These authors contributed equally to this work.
*Corresponding authors. Email: li.yu@iphy.ac.cn; htyang@iphy.ac.cn; dong@iphy.ac.cn

in-plane and out-of-plane superconducting coherence length and penetration depth are also deduced. We find that $H_{c1}(T)$ and SC diamagnetic signal change little initially below $T_c \sim 3.5$ K, and then increase abruptly upon cooling to a characteristic temperature ~2.8 K. A two-fold anisotropy in the in-plane angular-dependent magnetoresistance (AMR) is identified in the mixed state. Intriguingly, we find that, below the same characteristic $T \sim 2.8$ K, the orientation of the AMR anisotropy displays a twist by an angle of 60° characteristic of the Kagome lattice. Our findings shed new light on the emergence of superconductivity in the presence of the frustrated magnetism and intertwined orders.

The CsV_3Sb_5 single crystals were synthesized by the self-flux method.[13–15,23,27,29,30] The x-ray diffraction (XRD) data were collected at room temperature on a diffractometer (Rigaku SmartLab, 9 kW) equipped with two Ge (220) monochromators. The magnetic property measurements were conducted down to 1.8 K on a Quantum Design MPMS-XL1 system, and down to 0.4 K on an MPMS-3 system equipped with an iHe3 insert. The electrical transport properties were measured on a Quantum Design PPMS-9 system under magnetic fields up to 8 T.

The representative XRD pattern of the CsV_3Sb_5 single crystals, shown in the upper right inset in Fig. 1(a), confirms the single preferred (001) orientation. The lattice parameter c is calculated to be 9.318 Å, consistent with the previous reports.[23,30] The double-crystal x-ray rocking curve for the (008) Bragg reflection [Fig. 1(a)] demonstrates a small crystal mosaic of 0.24° in terms of the full width at half maximum (FWHM), indicating an excellent out-of-plane crystalline perfection. The x-ray ϕ-scan of the (202) plane in Fig. 1(b) displays six successive peaks with an equal interval of 60°, in accordance with the hexagonal symmetry of the Kagome lattice. The superconductivity of the CsV_3Sb_5 single crystals is confirmed by the superconducting diamagnetism at the onset $T_c \sim 3.5$ K as shown in Fig. 1(c), as well as by the zero resistance at ~3.0 K in Fig. 1(d). We note that the previous work usually reports a superconducting $T_c \sim 2.5$–2.8 K[13,17,21,23,24,31] in this Kagome system, which is lower than the T_c and zero-resistance temperature observed here in our samples. The higher T_c of our samples may be due to a sufficient content of the interlayer alkali atoms and almost stoichiometric V_3Sb_5 blocks containing the 2D Kagome lattice [see the upper left inset in Fig. 1(a)]. However, the superconducting transition is not as sharp as expected for our high-quality samples. It is noticeable in Fig. 1(c) that the diamagnetic signal gently sets in below ~3.5 K then abruptly drops around ~2.8 K, followed by a 100% superconducting shielding. Such a two-stage-like transition seems common in the CsV_3Sb_5 single crystals studied by different groups.[13,17,21,23]

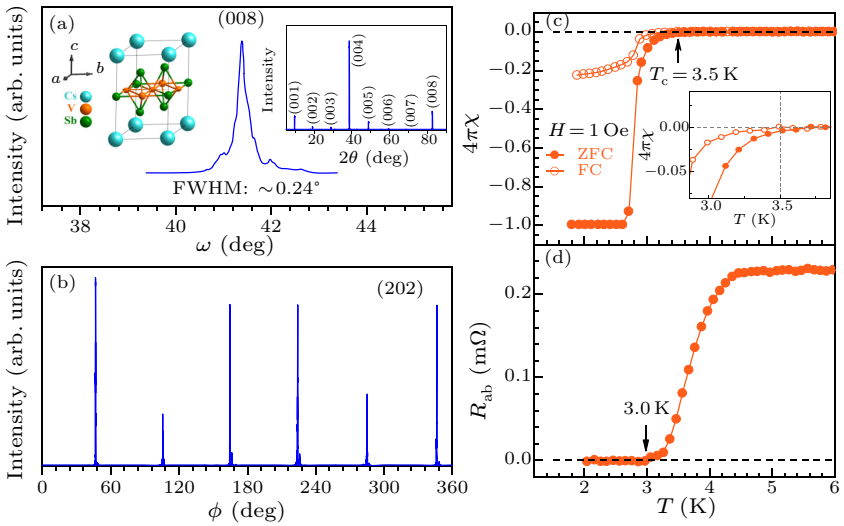

Fig. 1. Crystallographic and superconductivity characterizations of the CsV_3Sb_5 single crystal. (a) The x-ray rocking curve of (008) reflection shows a small FWHM of 0.24°. The left and right insets show the schematic crystal structure and x-ray θ–2θ scan, respectively. (b) The x-ray ϕ scan of the (202) plane. (c) The magnetic susceptibilities near the SC transition under zero-field cooling (ZFC) and field cooling (FC) modes. The magnetization data are corrected for the demagnetization factor. Inset: an enlarged view of the superconducting diamagnetic signals. (d) The temperature dependence of the in-plane resistance shows the zero resistance below ~3.0 K.

In order to obtain the upper critical field $H_{c2}(T)$ of the samples, the data of magnetoresistance $R(T)$ were collected under various fields along the c axis and ab plane. As shown in Figs. 2(a) and 2(b), the resistive transitions show no significant broadening in the magnetic fields. The temperature dependences of the obtained in-plane $H_{c2}^{ab}(T)$ and out-of-plane $H_{c2}^{c}(T)$ all show positive curvatures. Accordingly, the behav-

ior of $H_{c2}(T)$ is well fitted by a two-band model[32] rather than single-band WHH formula[33] [Fig. 2(c)], consistent with the multiband nature.[23,27] The zero-temperature $H_{c2}(0)$ is estimated to be 0.8 T for $H//c$ and 7.2 T for $H//ab$. The deduced in-plane coherence length is $\xi_{ab}(0) = 20.3$ nm, and the out-of-plane one $\xi_c(0) = 2.2$ nm. The anisotropic ratio $\gamma = \xi_{ab}/\xi_c \sim 9$, comparable with that of quasi-2D cuprate and iron-based superconductors.

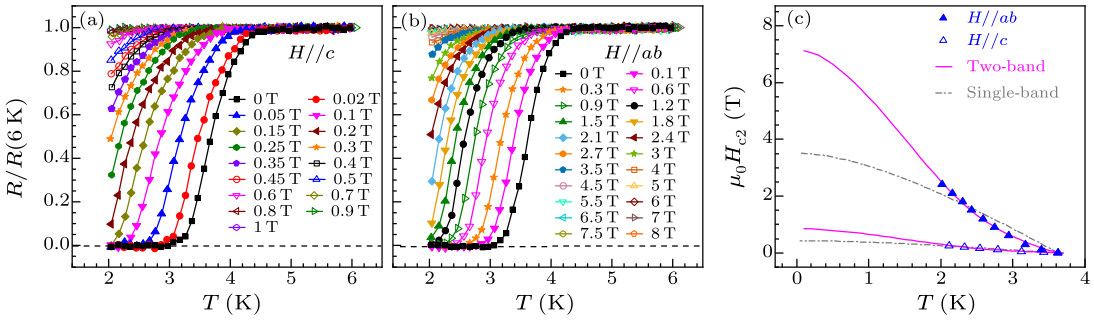

Fig. 2. The normalized resistance under magnetic fields and anisotropic upper critical magnetic fields of the CsV_3Sb_5 single crystal. [(a), (b)] Temperature dependences of normalized in-plane resistance measured under magnetic fields along the c axis and ab plane up to 8 T, respectively. (c) Temperature dependences of the upper critical fields, obtained from the $R(T)$ data [in (a) and (b)] at 50% of the normal-state resistance. The results of fitting by the two-band (pink solid curve) and single-band WHH (gray point-dashed curve) models are presented.

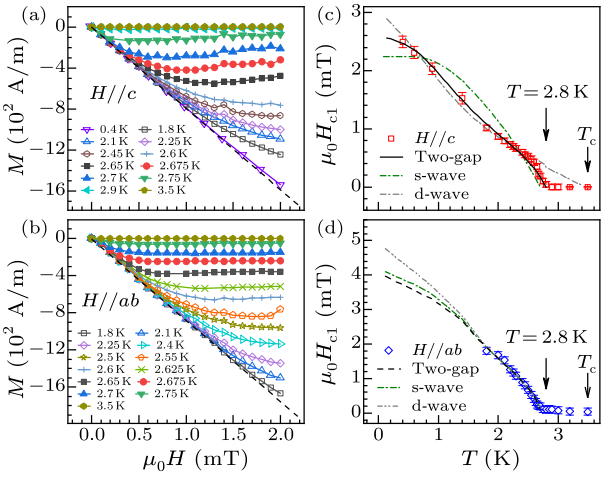

Fig. 3. The isothermal magnetization and anisotropic lower critical field of the CsV_3Sb_5 single crystal. [(a), (b)] The data of isothermal magnetization, corrected for the demagnetization factor, at various temperatures with magnetic field along the c axis and ab plane, respectively. [(c), (d)] The temperature dependences of $\mu_0 H_{c1}$ along the c axis and ab plane, respectively, defined as the fields at which M–H curves start to deviate from the Meissner line [$M/H = -4\pi$, the dashed lines in (a) and (b)]. The results of fitting by the two-gap, s-wave and d-wave models are also presented. The fittings for $H//ab$ via the three models shows no significant difference.

The measurements of lower critical fields $H_{c1}(T)$ can also provide important information of the multiband superconductivity in the Kagome metal CsV_3Sb_5. The results of isothermal magnetization $M(H)$ with magnetic field along the c axis and ab plane are presented in Figs. 3(a) and 3(b), respectively. The temperature dependences of the obtained H_{c1}^{c} and H_{c1}^{ab} are plotted in Figs. 3(c) and 3(d), respectively. The lower critical field shows unusual temperature dependence. As the system enters the superconducting state, both H_{c1}^{c} and H_{c1}^{ab} are nearly independent of temperature, corresponding to the gentle increase of diamagnetic signal with temperature [Fig. 1(c)]. Below the characteristic temperature $T \sim 2.8$ K, both H_{c1}^{c} and H_{c1}^{ab} rise abruptly with cooling, coinciding with the rapid increase in the Meissner and shielding signal sizes. The temperature dependences of H_{c1}^{c} and H_{c1}^{ab} are fitted by a semi-classical approach[34] with different models, including single band s-wave, d-wave and a simple two-gap one, as shown respectively in Figs. 3(c) and 3(d). Obviously, the two-gap model gives the best fit for $H_{c1}^{c}(T)$, yielding a London penetration depth $\lambda_{ab}(0) \sim 460$ nm, in agreement with that estimated by tunneling diode oscillator.[19]

It is noteworthy that the values of lower critical field H_{c1}^{ab} are higher than those of H_{c1}^{c}, which is reproducibly observed in our samples. This result of H_{c1} suggests that the in-plane effective electron mass (m_{ab}) is larger than the out-of-plane one (m_c). As suggested in theory,[11,12] the electronic physics in this material is likely driven by the Kagome–van Hove points. In this case, the effect of the electron-electron correlation becomes important and the band dispersion near Fermi energy can be strongly renormalized. Thus, combining the presence of van Hove physics and electron-electron correlation, the in-plane effective mass can be strongly enhanced.

To further investigate the unusual electronic and superconducting properties of the CsV_3Sb_5 system, the in-plane angular-dependent magnetoresistance was measured under a field of 0.5 T at different temperatures in the mixed state. As shown in Fig. 4(a), the AMR exhibits a pronounced *two-fold* rotational symmetry. To our knowledge, such an anisotropy in this system has never been reported before. To estimate the strength of relative change of the anisotropic

AMR signal, the ratios of $\Delta R/R_{\rm min} = [R(\theta,T) - R_{\rm min}(T)]/R_{\rm min}(T)\times 100\%$ are summarized in Fig. 4(b) by polar-coordinate plots. A large change of $\sim 50\%$ in AMR is observed, despite the quick reduction of the absolute values with lowering temperature, as shown in Fig. 4(a). This reflects the emergence of strong anisotropic scatterings under field in the mixed state of the CsV_3Sb_5 system.

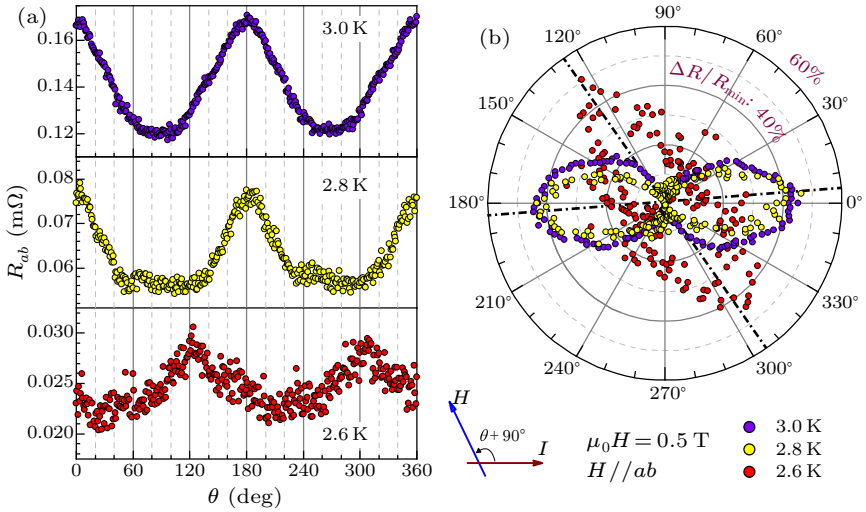

Fig. 4. The in-plane angular-dependent magnetoresistance (AMR) measured in the mixed state. (a) The AMR as a function of θ at $T = 3.0$, 2.8 and 2.6 K. Here θ is the angle between the directions of the external field (H) and the current (I), with $\theta = 0°$ corresponding to $H\perp I$, as illustrated by the schematic diagram. (b) Polar plots of $\Delta R/R_{\rm min} = [R(\theta,T) - R_{\rm min}(T)]/R_{\rm min}(T) \times 100\%$. The two-fold rotational symmetry in the AMR is obvious. The direction of the maximum AMR rotates by an angle of 60° below $T \sim 2.8$ K.

We note that significant two-fold anisotropy of the in-plane AMR has also been observed in a topological superconductor of trigonal $Sr_{0.10}Bi_2Se_3$ under a 0.4 T field in the mixed state.[35] In that case, however, the line shape of $R(\theta)$ changes significantly with temperature, which is distinct from our observation in CsV_3Sb_5 [Fig. 4(a)]. Furthermore, it is intriguing that, as the present hexagonal CsV_3Sb_5 is cooled below the characteristic temperature of $\sim$2.8 K, the direction of the maximum AMR rotates by an angle of 60° with respect to the original one, as shown in Figs. 4(a) and 4(b). Such a peculiar twist of the AMR orientation appears to coincide with the Kagome symmetry and its origin is not yet clear. Nevertheless, the anisotropic AMR and its mysterious rotation must relate to the complex electronic and crystallographic environments, which host the emergent anisotropic scatterings intertwined with certain coexisting orders and variable flux dissipation in the superconducting mixed state. The two-fold anisotropy in the mild in-plane field of 0.5 T and its high sensitivity to temperature imply a significant contribution from the spin degree of freedom and a weak coupling to the crystal lattice. Further investigation is certainly required for better understanding of the physics behind such an exotic rotation.

In summary, we report unusual superconducting properties observed in the high-quality single crystals of CsV_3Sb_5 with $T_c \sim 3.5$ K. Our experimental results are consistent with a quasi-2D multiband superconductor. The anisotropic lower critical field H_{c1} suggests a strongly renormalized in-plane effective mass, which indicates the presence of correlated electronic physics due to van Hove points near Fermi energy. We identify two-fold-anisotropic in-plane scatterings under a mild field of 0.5 T in the mixed state, and find a particular twist of 60° of the maximum-scattering direction below a characteristic temperature of $\sim$2.8 K. Moreover, we observe that both $H_{c1}(T)$ and SC diamagnetic signal show concurrent abrupt increases below the same characteristic temperature. These findings shed new light on the emergence of superconductivity in the presence of frustrated magnetism and intertwined orders in the Kagome lattice.

References

[1] Anderson P W 1973 *Mater. Res. Bull.* **8** 153
[2] Ran Y, Hermele M, Lee P A and Wen X G 2007 *Phys. Rev. Lett.* **98** 117205
[3] Balents L 2010 *Nature* **464** 199
[4] Lin Z, Choi J H, Zhang Q, Qin W, Yi S, Wang P, Li L, Wang Y, Zhang H, Sun Z, Wei L, Zhang S, Guo T, Lu Q, Cho J H, Zeng C and Zhang Z 2018 *Phys. Rev. Lett.* **121** 096401
[5] Yin J X, Zhang S S, Chang G, Wang Q, Tsirkin S S, Guguchia Z, Lian B, Zhou H, Jiang K, Belopolski I, Shumiya N, Multer D, Litskevich M, Cochran T A, Lin H, Wang Z, Neupert T, Jia S, Lei H and Hasan M Z 2019 *Nat. Phys.* **15** 443
[6] Ye L, Kang M, Liu J, Von Cube F, Wicker C R, Suzuki T, Jozwiak C, Bostwick A, Rotenberg E, Bell D C, Fu L, Comin R and Checkelsky J G 2018 *Nature* **555** 638
[7] Yin J X, Zhang S S, Li H, Jiang K, Chang G, Zhang B, Lian B, Xiang C, Belopolski I, Zheng H, Cochran T A, Xu

S Y, Bian G, Liu K, Chang T R, Lin H, Lu Z Y, Wang Z, Jia S, Wang W and Hasan M Z 2018 *Nature* **562** 91
[8] Liu E, Sun Y, Kumar N, Muechler L, Sun A, Jiao L, Yang S Y, Liu D, Liang A, Xu Q, Kroder J, Süß V, Borrmann H, Shekhar C, Wang Z, Xi C, Wang W, Schnelle W, Wirth S, Chen Y, Goennenwein S T B and Felser C 2018 *Nat. Phys.* **14** 1125
[9] Kang M, Ye L, Fang S, You J S, Levitan A, Han M, Facio J I, Jozwiak C, Bostwick A, Rotenberg E, Chan M K, Mcdonald R D, Graf D, Kaznatcheev K, Vescovo E, Bell D C, Kaxiras E, Van Den Brink J, Richter M, Prasad G M, Checkelsky J G and Comin R 2020 *Nat. Mater.* **19** 163
[10] Eric M K, Brenden R O, Chennan W, Stephen D W and Michael G 2021 *J. Phys.: Conden. Matter* (accepted)
[11] Tan H, Liu Y, Wang Z and Yan B 2021 arXiv:2103.06325 [cond-mat.supr-con]
[12] Feng X, Jiang K, Wang Z and Hu J 2021 arXiv:2103.07097 [cond-mat.supr-con]
[13] Ortiz B R, Teicher S M L, Hu Y, Zuo J L, Sarte P M, Schueller E C, Abeykoon A M M, Krogstad M J, Rosenkranz S, Osborn R, Seshadri R, Balents L, He J and Wilson S D 2020 *Phys. Rev. Lett.* **125** 247002
[14] Ortiz B R, Sarte P M, Kenney E M, Graf M J, Teicher S M L, Seshadri R and Wilson S D 2021 *Phys. Rev. Mater.* **5** 034801
[15] Yin Q, Tu Z, Gong C, Fu Y, Yan S and Lei H 2021 *Chin. Phys. Lett.* **38** 037403
[16] Wang Y, Yang S, Sivakumar P K, Ortiz B R, Teicher S M L, Wu H, Srivastava A K, Garg C, Liu D, Parkin S S P, Toberer E S, Mcqueen T, Wilson S D and Ali M N 2020 arXiv:2012.05898 [cond-mat.supr-con]
[17] Zhao C C, Wang L S, Xia W, Yin Q W, Ni J M, Huang Y Y, Tu C P, Tao Z C, Tu Z J, Gong C S, Lei H C, Guo Y F, Yang X F and Li S Y 2021 arXiv:2102.08356 [cond-mat.supr-con]
[18] Chen H, Yang H, Hu B, Zhao Z, Yuan J, Xing Y, Qian G, Huang Z, Li G, Ye Y, Yin Q, Gong C, Tu Z, Lei H, Ma S, Zhang H, Ni S, Tan H, Shen C, Dong X, Yan B, Wang Z and Gao H J 2021 arXiv:2103.09188 [cond-mat.supr-con]
[19] Duan W, Nie Z, Luo S, Yu F, Ortiz B R, Yin L, Su H, Du F, Wang A, Chen Y, Lu X, Ying J, Wilson S D, Chen X, Song Y and Yuan H 2021 arXiv:2103.11796 [cond-mat.supr-con]
[20] Jiang Y X, Yin J X, Denner M M, Shumiya N, Ortiz B R, He J, Liu X, Zhang S S, Chang G, Belopolski I, Zhang Q, Shafayat H M, Cochran T A, Multer D, Litskevich M, Cheng Z J, Yang X P, Guguchia Z, Xu G, Wang Z, Neupert T, Wilson S D and Zahid H M 2020 arXiv:2012.15709 [cond-mat.supr-con]
[21] Chen K Y, Wang N N, Yin Q W, Tu Z J, Gong C S, Sun J P, Lei H C, Uwatoko Y and Cheng J G 2021 arXiv:2102.09328 [cond-mat.supr-con]
[22] Du F, Luo S, Ortiz B R, Chen Y, Duan W, Zhang D, Lu X, Wilson S D, Song Y and Yuan H 2021 arXiv:2102.10959 [cond-mat.supr-con]
[23] Yu F H, Wu T, Wang Z Y, Lei B, Zhuo W Z, Ying J J and Chen X H 2021 arXiv:2102.10987 [cond-mat.str-el]
[24] Liang Z, Hou X, Ma W, Zhang F, Wu P, Zhang Z, Yu F, Ying J J, Jiang K, Shan L, Wang Z and Chen X H 2021 arXiv:2103.04760 [cond-mat.supr-con]
[25] Uykur E, Ortiz B R, Wilson S D, Dressel M and Tsirlin A A 2021 arXiv:2103.07912 [cond-mat.str-el]
[26] Li H X, Zhang T T, Pai Y Y, Marvinney C, Said A, Yilmaz T, Yin Q, Gong C, Tu Z, Vescovo E, Moore R G, Murakami S, Lei H C, Lee H N, Lawrie B and Miao H 2021 arXiv:2103.09769 [cond-mat.supr-con]
[27] Yang S Y, Wang Y, Ortiz B R, Liu D, Gayles J, Derunova E, Gonzalez-Hernandez R, Smejkal L, Chen Y, Parkin S S P, Wilson S D, Toberer E S, Mcqueen T and Ali M N 2020 *Sci. Adv.* **6** eabb6003
[28] Zhang Z, Chen Z, Zhou Y, Yuan Y, Wang S, Zhang L, Zhu X, Zhou Y, Chen X, Zhou J and Yang Z 2021 arXiv:2103.12507 [cond-mat.supr-con]
[29] Chen X, Zhan X, Wang X, Deng J, Liu X B, Chen X, Guo J G and Chen X 2021 arXiv:2103.13759 [cond-mat.supr-con]
[30] Ortiz B R, Gomes L C, Morey J R, Winiarski M, Bordelon M, Mangum J S, Oswald L W H, Rodriguez-Rivera J A, Neilson J R, Wilson S D, Ertekin E, Mcqueen T M and Toberer E S 2019 *Phys. Rev. Mater.* **3** 094407
[31] Zhao H, Li H, Ortiz B R, Teicher S M L, Park T, Ye M, Wang Z, Balents L, Wilson S D and Zeljkovic I 2021 arXiv:2103.03118 [cond-mat.supr-con]
[32] Gurevich A 2003 *Phys. Rev. B* **67** 184515
[33] Werthamer N R, Helfand E and Hohenberg P C 1966 *Phys. Rev.* **147** 295
[34] Prozorov R and Giannetta R W 2006 *Supercond. Sci. Technol.* **19** R41
[35] Pan Y, Nikitin A M, Araizi G K, Huang Y K, Matsushita Y, Naka T and De Visser A 2016 *Sci. Rep.* **6** 28632